Comparison of photoinduced reorientation of *ortho*-, *meta*-, and *para*-methyl red-doped nematic liquid crystals on rubbed polyimide

David Statman,[1] Ariel T. Statman,[2] Kaitlin Wozniak,[2] and Christopher Brennan[2]
[1]*Physics Department and Chemistry Department, Allegheny College, Meadville, Pennsylvania 16335, USA*
[2]*Physics Department, Allegheny College, Meadville, Pennsylvania 16335, USA*
(Received 26 May 2015; revised manuscript received 17 July 2015; published 28 August 2015)

We compare the photoinduced reorientation of the easy axis on rubbed polyimide surfaces for the nematic E7 doped with three isomers of methyl red; *ortho*, *meta*, and *para*. Using optical techniques, the angle and the pitch of the director at the polymer surface were measured before, during, and after photoexcitation of the dye. Optical absorbances were also measured before and after photoexcitation. Extrapolation lengths, hence anchoring energies, were determined with the on/off application of a magnetic field for *meta*- and *para*-methyl red-doped nematics. Because of an elastic reorientation of the easy axis in the presence of the magnetic field, we could not determine the extrapolation length of the *ortho*-methyl red-doped nematic. Our results confirm that photoinduced reorientation is facilitated by desorption of all dyes from the polymer surface. While there is little evidence of weak photoinduced adsorption of *meta*- and *para*-methyl red to the surface during photoexcitation, there is strong evidence of photoinduced adsorption of *ortho*-methyl red, which is long lasting.

DOI: 10.1103/PhysRevE.92.022503 PACS number(s): 42.70.Df, 42.70.Gi

I. INTRODUCTION

Nematic liquid crystals doped with azobenzene (*azo*) dyes facilitate an enhancement of the optically induced reorientation of the liquid crystal director. This enhancement is achieved via photoexcitation of the dye, normally in the *trans* conformation, sometimes with subsequent isomerization to the *cis* conformation. Early work has demonstrated that this enhancement is, in part, the result of a bulk effect, where it has been suggested that an asymmetric distribution of *trans*, *cis*, and excited state dye molecules exert a torque both through a molecular field [1] and diffusion asymmetry [2,3]. This torque is proportional to the intensity of light incident on the sample.

For some *azo* dye-doped samples the magnitude of the enhancement is such that reorientation of the liquid crystal director cannot be explained by the bulk effect alone. Evidence exists of photoinduced reorientation of the easy axis at the liquid crystal–polymer surface [4,5]. For example, it has been observed that liquid crystal samples doped with the *azo* dye *ortho*-methyl red and with one surface coated with fluorinated polyvinyl cinnamate (PVCN-F) demonstrate a significant amount of reorientation of the easy axis on that surface [6–11]. While Andrienko *et al.* [12] argue that this reorientation is the result of the transfer of angular momentum from the light to the dye, Lucchetti *et al.* [11] observed what they referred to as sliding on similar samples irradiated with circularly polarized light. The sliding was always in the same direction regardless of the handedness of the polarization of the light leading to the conclusion that transfer of angular momentum is not significant and that the reorientation is a surface effect. They describe this effect as a surface induced nonlinear effect (SINE) [13] arising from photoinduced modifications of the anchoring conditions. It has been proposed that these modifications can be explained by the photoinduced desorption of the *trans* isomer from the polymer surface and photoinduced adsorption of the dye back onto the surface [14]. Results of Fedorenko *et al.* [8] and Dubtsov *et al.* [15] support this argument. In addition, Lucchetti *et al.* [16] have reported colossal optical nonlinearities when a low-frequency electric field is applied to methyl red-doped nematics. Considering the observation by Pagliusi *et al.* [17] that there is a buildup of electric charges near the electrodes reducing the effective voltage drop across the sample, they suggest that photoinduced desorption of dye molecules impacts the density of surface charges that screen an applied field. Most recently, Lucchetti and Simoni [18] compared the effects of applied dc and ac fields, and of changing the polarity of the dc field. They argue that negative charge complexes, in fact, are involved in the light-induced desorption and adsorption process, and that both the transient responses and the light-induced permanent anchoring have the same origin. In addition, their results indicate that the role of *trans* to *cis* isomerization is limited.

This photoinduced reorientation of the easy axis can be compared with the gliding of the easy axis observed when an external torque is applied via an electric or magnetic field to an undoped liquid crystal [6,19–21]. In that case, both azimuthal (in-plane) and zenithal (out-of-plane) gliding for undoped nematics have been observed [19,22]. While such gliding is most prominent on soft polymer surfaces, such as polymethyl methacrylate (PMMA), it has also been reported to occur on hard polymer surfaces such as polyimide (PI) [20,22]. Various workers have suggested that for undoped nematics, this gliding of the easy axis might also be the result of adsorption and desorption of the liquid crystal on the polymer surface [7,8]. Other explanations include a mutual reorienting of the liquid crystal and polymer network [6,19,20], or the existence of sublayers with different physical properties near the polymer surface [23,24]. One characteristic of this type of gliding is that it is not only slow, but appears to be plastic. Upon removal of the external torque, the easy axis does not immediately return to its original orientation. That return can take hours or days, and is probably the result of the bulk liquid crystal molecules exerting a torque to bring the easy axis back to its original orientation.

While many of the reports of photoinduced reorientation of the easy axis involve the dye methyl red on PVCN-F, it has also been observed on other polymer surfaces. Lucchetti and Simoni recently reported photoinduced reorientation of

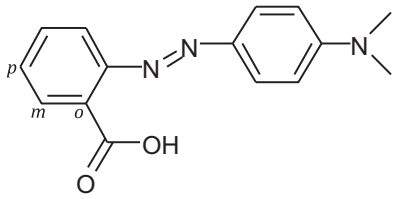

FIG. 1. Structure of *ortho*-methyl red. *o*, *m*, and *p* refer to the *ortho*, *meta*, and *para* sites on the phenyl ring.

the easy axis on cells without any special coating [18]. We have also measured photoinduced reorientation of the easy axis on both rubbed PI and unrubbed polymethyl methacrylate [5], confirming that photoexcitation of *azo* dyes in nematics induces easy axis reorientation on rubbed PI as well as other polymers. We have found that this also involves a *memory* effect, consistent with the results of Ouchi *et al.* [25]. In particular, for a series of measurements, the amount of reorientation increased with each subsequent measurement. In addition, we found that illumination of the sample with circularly polarized light increased the amount of subsequent reorientation by several times. This appears to support the photoinduced desorption and adsorption hypothesis.

In this paper, we continue this study of the photoinduced reorientation of the easy axis for methyl red-doped nematics on polyimide surfaces. In particular, we are interested in comparing the behaviors of three methyl red isomers, *ortho*, *meta*, and *para*, where the designation corresponds to the position of the carboxyl group on the phenyl ring, as shown in Fig. 1. Quantum mechanical calculations [26] indicate that all three isomers are planar as neutral species, meaning the dihedral angle between the phenyl rings is zero. However, the planarity of the *ortho* dye is stabilized by *intramolecular* hydrogen bonding, which does not occur in the other two dyes. In the absence of hydrogen bonding, such as when *ortho*-methyl red is in the anionic form, the dihedral angle is calculated to be 30°. However, the *meta* and *para* dyes remain planar when in the anionic form, as indicated by quantum chemical calculations. As opposed to the *ortho* dye, these dyes are only capable of *intermolecular* hydrogen bonding. In other words, the molecular orbitals describing the *meta* and *para* dyes are symmetrically different from those of the *ortho* dye, indicating different chemistries. The question we ask is how photoinduced reorientation of the easy axis differs for the three dyes.

Although many studies involved cells consisting of a reference surface coated with the rubbed polyimide (PI), which is known to strongly anchor, and a test surface coated with fluorinated polyvinyl cinnamate (PVCN-F) or just polyvinyl cinnamate (PVCN) [6–17], in this study we coated both surfaces with rubbed polyimide. As mentioned, Lucchetti and Simoni [18] have shown that photoinduced reorientation of the easy axis does not need any special coating. In our case there is no need for specially prepared reference or test surfaces, as we are interested in photoinduced reorientation on rubbed PI. As we will discuss, a reference surface is, nevertheless, maintained. In Sec. II we describe our experiment. In Sec. III we present results and discussion, with conclusions in Sec. IV.

II. EXPERIMENT

Dyed thermotropic liquid crystal samples (E7) were prepared at concentrations of 0.2% (dye–liquid crystal) by weight. Cleaned glass microscope slides were spin coated with polyamic acid and cured to PI in an oven. Uniformity of coating was determined from optical interference. Cured PI slides were rubbed with velvet. Cells were constructed using 20-μm spacers. In constructing the cells, the rubbing directions of the slides were slightly misaligned, thereby allowing a small initial twist in the director. This was done for calibration purposes, as will be described later. Epoxy was used to cement slides together and they were held together with clamps while curing. The cell path lengths were then determined interferometrically in the red-infrared end of the spectrum, as we could not get interference fringes with reasonable visibility at the blue-green end of the spectrum. Typically the cells were found to be between 15 and 18 μm in length with a standard deviation on the order of 0.2 μm. This standard deviation is consistent with an optical flatness on the order of $\lambda/4$ at the blue-green end of the spectrum. In this study, our cell thicknesses were slightly smaller than the spacers, probably because of our clamping procedure.

Cells were filled with the dyed nematics and examined under a cross-polarized microscope to determine both quality of alignment and the twist angle. The pitch was calculated as the cell thickness divided by the twist angle. Using an Ocean Optics spectrometer, the absorption spectra of the samples were taken both before and after the photoinduced reorientation experiment.

The anchoring energy was measured, using a technique adapted from that developed by Jánossy [27], in an experimental setup shown in Fig. 2 and described elsewhere [5]. The sample was placed between poles of an electromagnet, oriented so that the magnetic field, when applied, was approximately perpendicular to the initial orientation of the director and parallel to the plane of the sample. The magnetic field strength was set at 0.2 T. A probe beam, from a white light source and filtered to exclude any light that might induce photoexcitation of the dye, was polarized parallel to the rubbing direction on the entrance face of the sample and passed through the sample. As explained by Jánossy [27], the probe must be from an incoherent source and the length of the sample must be long enough to avoid interference effects between the ordinary and extraordinary polarizations. The polarization state of the exiting probe, as described by the Stokes parameters, was measured by passing the signal through the photoelastic modulator (PEM-100, Hinds Instruments) and then through an analyzer whose polarization was oriented 45° to the initial polarization of the probe. The second harmonic signal from the PEM gave the second Stokes parameter, which, as shown by Jánossy [27], is proportional to the polarization angle, θ, of the exiting beam. This, in the Mauguin limit, is the orientation of the director, φ, at the exit surface. The sample was rotated so that the initial second harmonic signal was zero. The signal was then calibrated by measuring the second harmonic signal as the PEM was rotated through $\pm 2°$. While ideally it would have been better to rotate the analyzer along with the PEM, this was logistically not possible, as the PEM and the analyzer could not be placed on the same

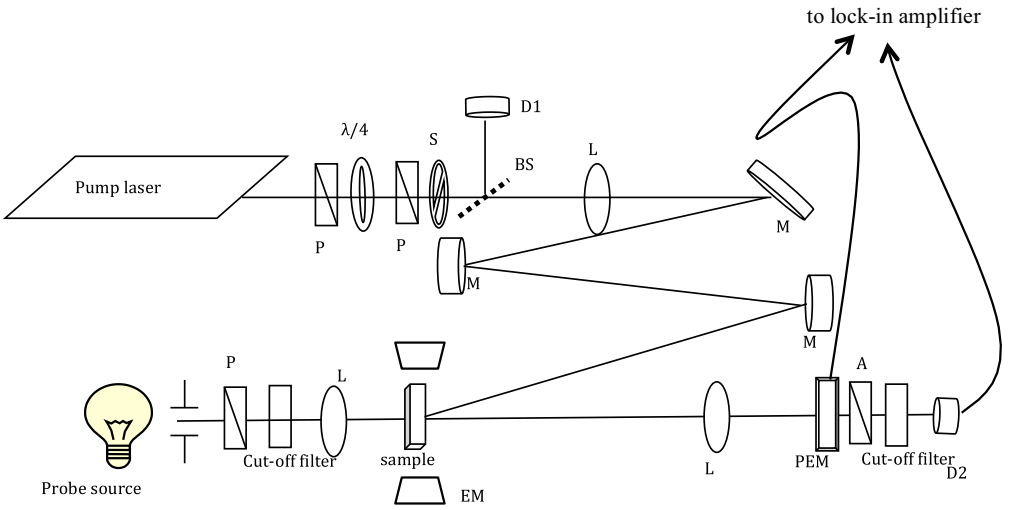

FIG. 2. (Color online) Experimental design. P: polarizer; BS: beam splitter; D1: pump input detector; D2: signal detector; L: lens; EM: electromagnet: PEM: photoelastic modulator; M: mirror; S: shutter; A: analyzer. The applied magnetic field is parallel to the plane of the sample and perpendicular to the probe beam.

mount. However, we were able to determine that for such a small rotation, any impact was negligible. The initial twist angle of the director was included in this calibration. To account for the initial twist to the director, it was added to the angle determined from the second harmonic signal during data analysis. The first harmonic signal from the PEM gave the third Stokes parameter, which, as shown by Jánossy [27], is inversely proportional to the pitch of the liquid crystal at the exit surface. For simplicity, we will refer to the inverse of the pitch as the *twist*, so the first harmonic signal is proportional to this *twist*. The first harmonic signal was calibrated to the initial twist. In general, we found that this calibration was consistent between samples with different initial twists, indicating that any offset in the signal from possible impact of other optical components was negligible. This method of determining both the orientation and twist of the director at the exit face is very sensitive to small changes in angle and in twist. It also includes whether the angle and twist are negative or positive in our experimental reference frame. The director angle and twist at the exit face were measured during a sequence in which the magnetic field was turned on and off. As will be explained in the Results section, the extrapolation length, which is inversely proportional to the anchoring strength, was calculated by taking the ratio of the change in the director angle to the change in the twist, $\Delta\varphi/\Delta\varphi'$, as the magnet is turned on and off. As shown by Jánossy [27], this ratio and its relationship to the extrapolation length at the probe exit is independent of whether the easy axis at the probe entrance also undergoes some photoinduced reorientation.

Photoinduced azimuthal reorientation of the easy axis was achieved using an Ar^+ laser tuned to the 488-nm line and polarized at an angle of $+45^\circ$ with respect to the initial polarization of the probe beam. The pump-probe configuration with the pump and probe beams entering the sample from opposite faces, the pump polarization at 45° to the initial polarization of the probe beam, and the probe beam parallel to the director at the probe entrance are the same as that described in our previous work, as well as in the most recent work of Lucchetti and Simoni [18]. The laser was set to a power of 15 mW and was collimated to have an irradiance of $16\,\mathrm{mW/cm^2}$ at the sample. Before, during, and after irradiation, the director angle and the twist at the probe exit was measured while the magnetic field was repeatedly turned on and off. Typical results are shown in Figs. 3–5.

Even though attenuation of the pump beam as it propagates through the sample is not large, we do not observe significant reorientation of the easy axis at the probe entrance. With the pump entering the sample at the probe exit with a polarization 45° to the director, the birefringent nematic sample initially behaves as a phase retarder. Because the cell thicknesses have

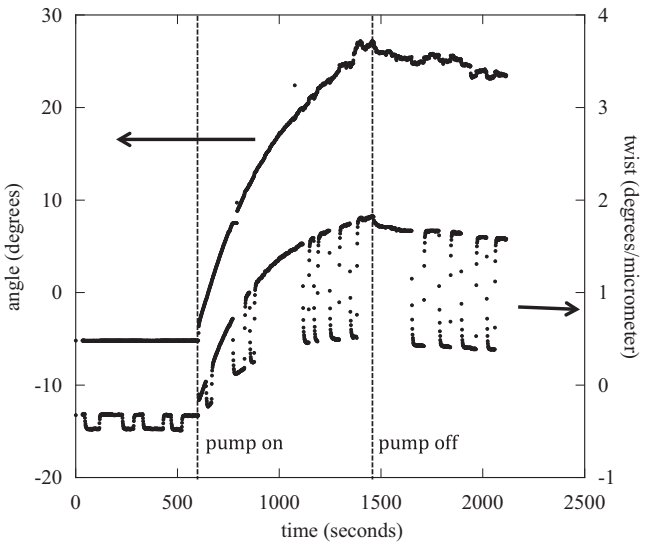

FIG. 3. *Ortho*-methyl red-doped sample: Director angle and twist (1/pitch) in degrees and degrees/μm. The twist becomes more negative (or decreases when the twist is positive) when the magnetic field is applied, and it becomes more positive when the magnetic field is removed.

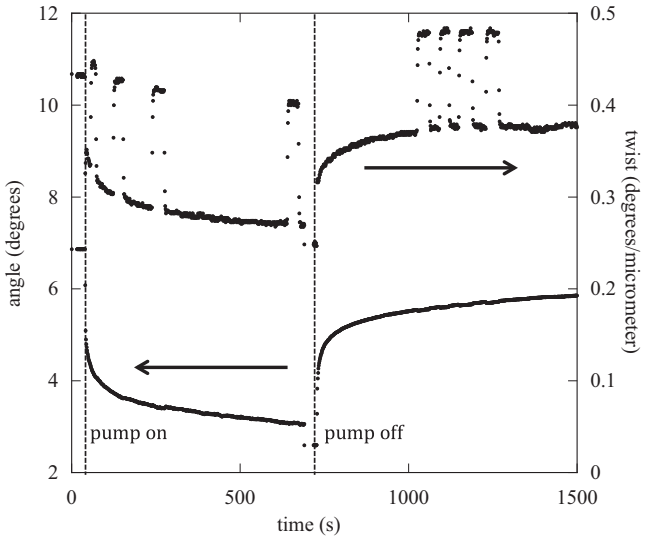

FIG. 4. *Meta*-methyl red-doped sample: Director angle and twist (1/pitch) in degrees and degrees/μm. The twist becomes more positive when the magnetic field is applied, and it becomes more negative when the magnetic field is removed.

a standard deviation on the order of $\lambda/2$ and the pump beam diameter is relatively large, at the surface of the probe entrance the pump is randomly polarized and cannot induce significant reorientation. Subsequent reorientation of the director at the probe exit results in the nematic being twisted. If that reorientation were large enough, the polarization of the pump would no longer be randomized. Rather it would be elliptical, and, in the Mauguin limit, its major axis would follow the director as it propagates through the sample. Therefore, even though we have observed photoinduced reorientation on strongly anchoring surfaces such as rubbed polyimide, there is still very little reorientation of the easy axis at the probe entrance. That cell surface still acts as a reference surface, similar to that in previous studies.

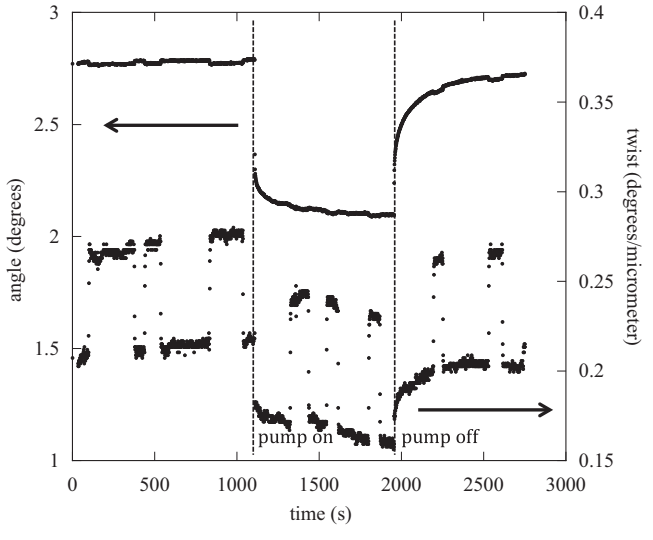

FIG. 5. *Para*-methyl red-doped sample: Director angle and twist (1/pitch) in degrees and degrees/μm. The twist becomes more positive when the magnetic field is applied, and it becomes more negative when the magnetic field is removed.

III. RESULTS AND DISCUSSION

We observe photoinduced reorientation of the director at the *rubbed* polyimide surfaces for all three dyed samples. However, as can be seen in Figs. 3–5, the *ortho* dye-doped nematic behaves differently than *meta* and *para* dye-doped nematics. Most obvious is that while the director of *ortho* dye-doped nematic rotates *toward* the pump polarization by as much as 30° or more, the directors of the *meta* and *para* dye-doped nematics rotate *away from* the pump polarization and only by about 4° and less than 1°, respectively. Although what is significant is that the qualitative observation that the rotation of the director for the *ortho* isomer is much greater than that of the *meta* and *para* isomers, we were able to confirm that the rotation angles measured for the *ortho* were reasonably accurate by subsequently measuring them using a polarizing microscope. While not shown in these figures, often the *ortho* dye-doped nematic exhibits an initial transient rotation away from the pump polarization before rotating toward the pump polarization. This behavior of the *ortho* dye-doped nematic is consistent with the results and interpretation of Fedorenko *et al.* [10], Ouskova *et al.* [14], and Lucchetti and Simoni [18]. Lack of evidence of rotation reversal toward the pump polarization for the *meta* and *para* dye-doped nematics would suggest that if photoinduced adsorption occurs in these samples, it is not significant. Although the 488-nm absorption cross sections of the *meta* and *para* dye-doped nematics are smaller than that of the *ortho* dye-doped nematic by a factor of 2–3 (cf. Figs. 9–11), since the *meta* and *para* isomers show considerable relaxation of the photoinduced director rotation once the pump is turned off and since relaxing species enter the rate equations, we do not believe that the smaller cross sections can explain why, in these samples, the director continues to rotate away from the polarization, does not change rotation direction, and does not exhibit such a large reorientation. Therefore, consistent with the arguments of Lucchetti and Simoni, smaller cross sections should only result in a change in the rate of reorientation and not the rotation direction [18]. We also see that while none of the directors of the three dye-doped nematics return to their original orientation, this quasipermanent reorientation is much more significant and longer lived for the *ortho* dye-doped nematics.

For all three dye-doped nematics the photoinduced change in director angle, φ, is associated with a change in the orientation of the easy axis at the polymer surface. It can be shown that the relationship between the director angle and twist at the surface is determined by the balance of torques and given by

$$\varphi' = -\frac{1}{2\xi}\sin\left[2(\varphi-\varphi_E)\right] = -\frac{1}{\xi}(\varphi-\varphi_E). \qquad (1)$$

where $\varphi' = d\varphi/dz$ is the twist, $\xi = K_{22}/W$ is the extrapolation length with W the anchoring strength and K_{22} the Frank constant, and φ_E is the azimuthal angle of the easy axis. Since the anchoring strength and the Frank constant are both positive, the extrapolation length must also be positive. Equation (1) therefore predicts that if the easy axis is not rotating, the

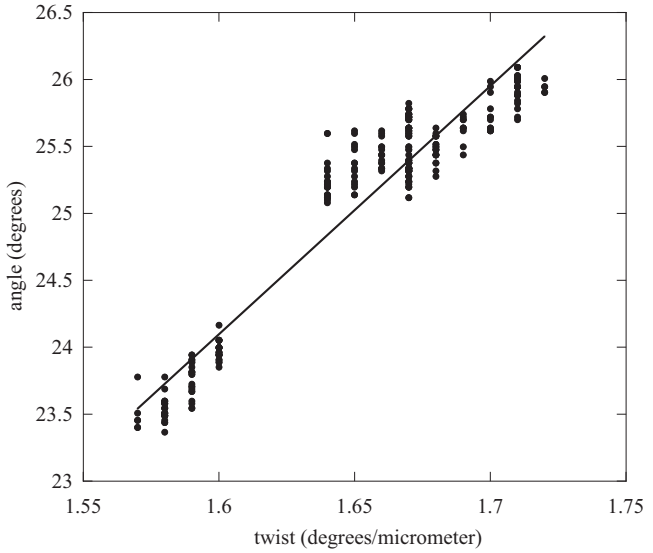

FIG. 6. *Ortho*-methyl red-doped sample immediately after irradiation. Director angle versus twist. Data are fit to $\phi = a + b\phi'$; $a = -5.560^\circ$, and $b = 18.54\,\mu$m. $R^2 = 0.919\,45$.

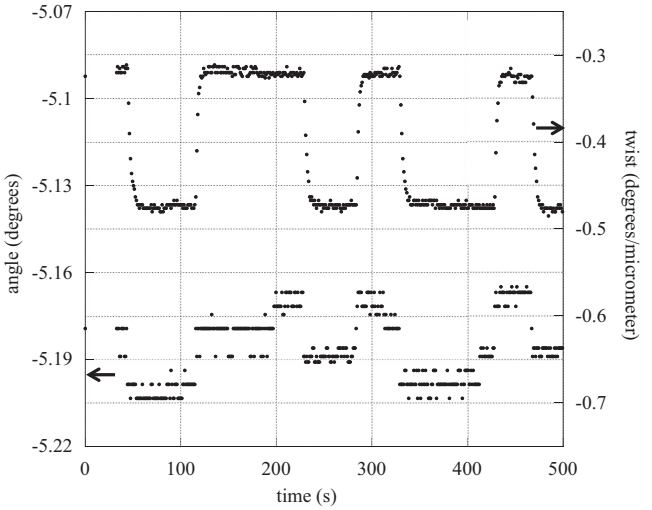

FIG. 7. *Ortho*-methyl red-doped sample before irradiation. Director angle and twist (1/pitch) in degrees and degrees/μm. The twist and the angle become more negative when the magnetic field is applied, and they become more positive when the magnetic field is removed.

director angle at the surface and the twist must change in opposite directions, $d\varphi = -\xi d\varphi'$. The director angle and the twist both changing in the same direction is evidence that the easy axis itself must be rotating. Figures 3–5 confirm the photoinduced change in easy axis for all three samples, as the director angle and the twist both change in the same direction when the pump beam is turned on.

Comparisons of the director angle and the twist at the probe exit for all three samples show that there is some photoinduced reorientation of the director at the probe entrance, but that it is quite small and significantly less than that at the probe exit. This is indicated by plots of the director angle versus the twist for all three samples when the pump is subsequently turned off and there is no applied magnetic field, an example of which is shown in Fig. 6 for the *ortho* dye-doped sample. All plots give negative intercepts, and, within an experimental uncertainty that varies between 10% and 50% depending on the sample, slopes that are on the order of the cell thickness. For the *meta* and *para* dye-doped samples, the final twist after photoinduced reorientation of the easy axis was too small to measure under a polarizing microscope. Measurement of the final twist of the *ortho* dye-doped sample under a polarizing microscope was consistent with our plots of the director angle and twist such as that shown in Fig. 6.

Another significant difference between the *ortho* dye-doped nematic and the *meta* and *para* dye-doped nematics is shown in Figs. 7–9. These figures give a closeup view of the director angle and twist at the probe exit as the magnetic field is turned on and off before the pump is applied. To interpret these figures, it is important to note that the initial director angle at the probe entrance is 0°. The magnetic field is approximately perpendicular, however, to the initial director angle at the probe exit. Therefore, with respect to the director at the probe entrance, the magnetic field is oriented at angles of about 85°, 97°, and 93° for the *ortho*, *meta*, and *para* dye-doped nematic samples, respectively. In other words, in the bulk, we would expect the magnetic field to rotate the director in the positive direction for the *ortho* dye-doped nematic, and in the negative direction for the *meta* and *para* dye-doped nematic. All things being equal, these differences, which are only a consequence of cell construction, should not have any impact on our results or their interpretation.

These figures show that the angle and twist of the *meta* and *para* dye-doped nematics change in opposite directions with the application of the magnetic field. On the other hand, the angle and the twist of the *ortho* dye-doped nematic change in the same direction. At the probe exit, both the director angle

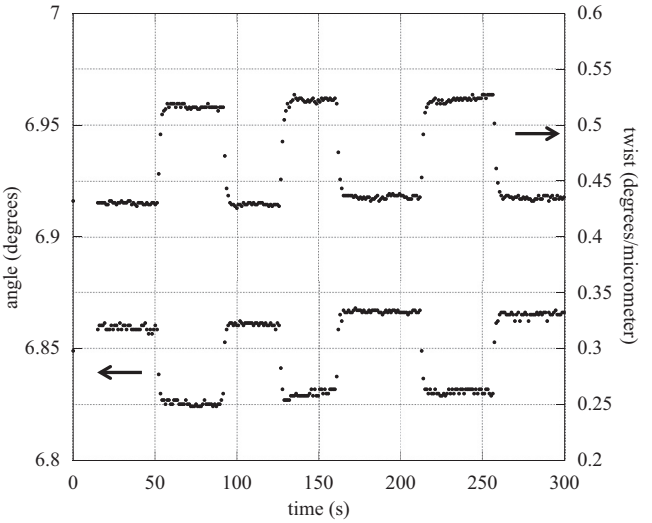

FIG. 8. *Meta*-methyl red-doped sample before irradiation. Director angle and twist (1/pitch) in degrees and degrees/μm. The twist increases and the angle decreases when the magnetic field is applied. The twist decreases and the angle increases when the magnetic field is removed.

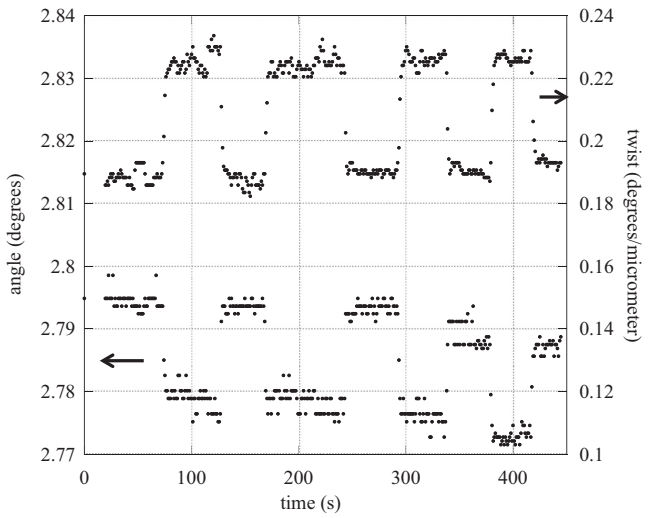

FIG. 9. *Para*-methyl red-doped sample before irradiation. Director angle and twist (1/pitch) in degrees and degrees/μm. The twist increases and the angle decreases when the magnetic field is applied. The twist decreases and the angle increases when the magnetic field is removed.

and the twist for the *ortho* dye-doped nematic become more negative in the presence of the magnetic field. According to Eq. (1) and the previous discussion, the magnetic field must therefore be responsible for a torque not just on the director, but also on the easy axis of the *ortho* dye-doped nematic resulting in its rotation even before any photoinduced reorientation. This cannot be the result of any photoinduced effects on the entrance surface, as the measurement only corresponds to changes with the application of the magnetic field. This rotation is not the same as the gliding observed when a magnetic field is applied to an undoped nematic on a soft polymer [6,19–24]. It is *elastic*. The easy axis returns to its original orientation when the magnetic field is removed. The ratio of the change in director angle to the change in twist, $\Delta\varphi/\Delta\varphi'$, is calculated to be $0.14 \pm 0.04\,\mu$m, which is much smaller than the cell length. Therefore, the torque applied by the magnetic field on the easy axis at the probe exit must be in the opposite direction to the torque applied by the magnetic field on the director in the bulk nematic. There is little evidence that the magnetic field facilitates a similar elastic rotation on the *meta* and *para* dye-doped nematics.

Elastic rotation for the *ortho* dye-doped nematic in the presence of the magnetic field continues during photoexcitation of the dye. When the pump is applied, as shown in Fig. 3, both the director angle and the twist at the probe exit become positive and quite large with a ratio slightly less than the cell length. When the magnetic field is applied, both the director angle and the twist at the probe exit decrease. Just as before the application of the pump, the ratio $\Delta\varphi/\Delta\varphi'$ is significantly less than the length of the cell, changing from $0.25 \pm 0.08\,\mu$m to $0.08 \pm 0.04\,\mu$m. Therefore, the torque on the easy axis at the probe exit continues to be in the opposite direction of the torque on the director in the bulk nematic. The decrease in the director angle at the probe exit indicates that the torque, hence the elastic rotation of the easy axis at the probe exit, is away from the magnetic field. When the pump is turned off, the director angle at the probe surface decreases slightly, cf. Fig. 3. With the application of the magnetic field, the ratio $\Delta\varphi/\Delta\varphi'$ remains positive and increases to $0.4 \pm 0.1\,\mu$m. Again, the elastic rotation is away from the magnetic field.

For both the *meta* and *para* dye-doped nematics, the director angle and the twist at the probe exit change in opposite directions, as seen in Figs. 8 and 9. If there is any elastic rotation of the easy axis in the presence of the magnetic field, it is very weak. Therefore Eq. (1) can be used to estimate the extrapolation length for the *meta* and *para* dye-doped nematics, by considering that if the easy axis angle, φ_E, does not change significantly during the application of the magnetic field, then the extrapolation length is given by

$$\xi = -\frac{\Delta\varphi}{\Delta\varphi'}. \tag{2}$$

The extrapolation lengths for the *meta* and *para* dye-doped nematics before, during, and after irradiation are given in Table I. Unfortunately we cannot determine the extrapolation length for the *ortho* dye-doped nematic because of the elastic rotation of the easy axis in the presence of a magnetic field. Table I also lists estimated anchoring strengths of the *meta* and *para* dye-doped nematics based on a value of 7.35 pN for K_{22} [28]. These values can be compared with azimuthal anchoring strength of $160\,\mu\text{J/m}^2$ for E7 on rubbed polyimide, as reported by Yu *et al.* [28]. From Table I, it can be seen that before irradiation, the anchoring strengths are less than that reported in the literature. During irradiation by the pump, the extrapolation length decreases and the anchoring strengths start to approach that of E7 on polyimide in the absence of adsorbed dye. When the pump is turned off, the extrapolation length increases and the anchoring strengths decrease, although they do not appear to return to their original values for the *meta* dye-doped nematic.

Before and after optical absorbance spectra of the dye-doped nematics, shown in Figs. 10–12, indicate that the dyes exist in equilibrium mixtures of the anionic and the neutral forms. For all three dyes, the optical absorbance of the anionic form occurs between 425 and 450 nm and has a smaller cross section than the optical absorbance of the neutral form, which occurs between 525 and 550 nm [29,30]. These spectra indicate that the anionic form of the dye is dominant in the *meta*

TABLE I. Extrapolation length and anchoring energy (assuming $K_{22} = 7.35$ pN) for dye-doped nematics.

	$\xi(\mu\text{m})$, $\text{W}(\mu\text{J/m}^2)$		
Dye	Before	During	After
Meta-methyl red	$0.40 \pm 0.02,\ 18 \pm 1$	$0.06 \pm 0.03,\ 120 \pm 60$	$0.24 \pm 0.03,\ 31 \pm 4$
Para-methyl red	$0.22 \pm 0.04,\ 33 \pm 6$	$0.11 \pm 0.03,\ 67 \pm 18$	$0.20 \pm 0.03,\ 37 \pm 5$

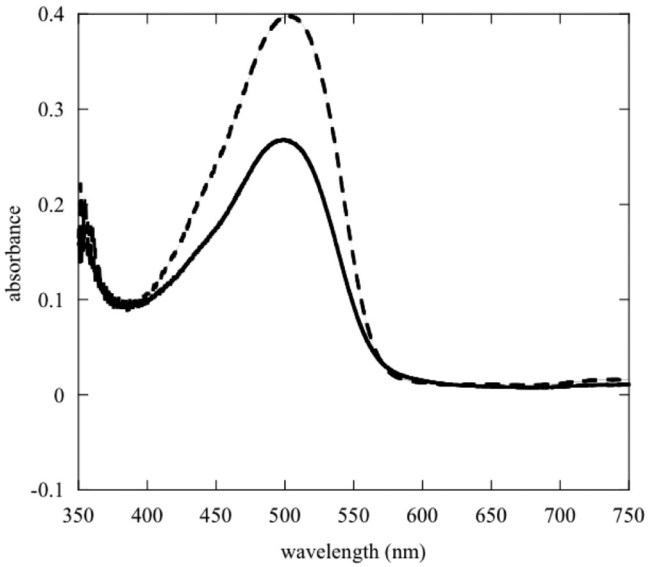

FIG. 10. Absorbance spectra of *ortho*-methyl red before (dash) and after (solid) photoexcitation.

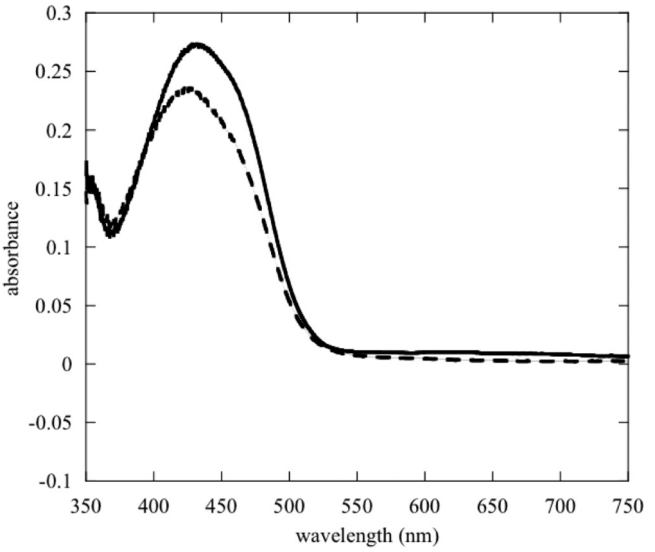

FIG. 11. Absorbance spectra of *meta*-methyl red before (dash) and after (solid) photoexcitation.

and *para* dye-doped nematics. The *ortho* dye-doped nematic, however, shows a more equal mix of the anionic and neutral forms of the dye. This is probably because intramolecular hydrogen bonding stabilizes the neutral form. The shoulder at 440 nm, however, confirms the presence of the anionic form.

After photoinduced reorientation, the absorbance of the *ortho* dye-doped nematic is significantly decreased and slightly shifted to the blue, as seen in Fig. 10. This indicates an increase in the amount of dye present in the anionic form. The decrease in absorbance can be seen visually as a bleached hole in the sample, which has a diameter of about 1.1 cm (same as that of the pump beam). In fact, it typically takes several months to a year or so for this hole to disappear, and for the *ortho* dye-doped nematic sample to return to its original absorbance spectrum as well as its original director orientation. Back of the envelope calculations show that there are about 30 layers of dye molecules per micrometer of optical path length. For the observed 35%–40% change in absorbance in the *ortho* dye-doped sample, about ten to 11 layers of dye within a micrometer length, or 180–200 layers within a typical sample, would need to be affected. This does seem to be rather large as a surface effect, suggesting that most of the decrease and shift in optical absorbance observed only in the hole occurs in the bulk. Yet under the microscope we observe neither spreading nor change of shape of the hole over the course of several months. The hole appears to be semipermanent. Therefore, we are inclined to believe that there is very little, if any, translational diffusion, as otherwise the diffusion coefficient would be incredibly small. We suggest that the change in the absorbance of the *ortho* dye-doped nematic is the result of a photophysical or photochemical surface effect during the photoexcitation process, which may well extend into the bulk dye in the vicinity of the affected surface.

The optical absorbance band corresponds to the $n \rightarrow \pi^*$ transition. This involves moving the lone pair electrons on the nitrogen atoms into the π^* antibonding orbital, making them no longer available for hydrogen bonding. It is likely that such a transition weakens the intramolecular hydrogen bonding, allowing for the ionization of the dye molecule. Apparently the anionic dye molecule in the excited state strongly adsorbs to the polymer surface. In other words, during photoexcitation *ortho* dye molecules are ionized and, if near the polymer surface, strongly adsorbed to that surface.

Contrast the behavior of the *ortho* dye-doped nematics with the *meta* and *para* dye-doped nematics where we observe a spectral shift to the blue with an increase in the absorbance, cf. Figs. 11 and 12. This spectral shift is localized to the region where photoexcitation occurs, with little evidence of diffusion. It is comparatively short lived. This suggests that during photoexcitation, the anionic form of the dye desorbs from the surface, leaving room for neutral forms. Readsorption of the anionic form to the surface does not

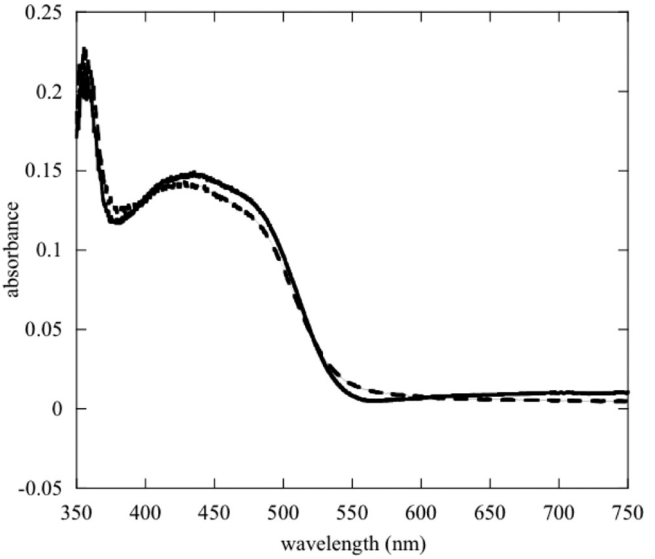

FIG. 12. Absorbance spectra of *para*-methyl red before (dash) and after (solid) photoexcitation.

appear to occur to any significant extent until after the pump is removed.

IV. CONCLUSION

It is well known that azobenzene dyes are responsible for photoinduced reorientation of the director for nematic liquid crystals. While some of the reorientation occurs in the bulk, it has been clear that surface effects play an important role in this effect. Previous work has shown that when the azobenzene dye is *ortho*-methyl red, these surface effects involve negatively charged species [16–18]. We have extended this work to include *meta*- and *para*-methyl red. For all three isomers of methyl red, we have identified the negative species as the anionic, or basic form of the dyes.

Our results show that for all three isomers, during photoexcitation of the dye, anionic dye molecules previously adsorbed to the surface are desorbed. For the *meta* and *para* isomers, desorption of anionic dye molecules is confirmed by a redshift in the absorbance spectra, and is accompanied by an increase in the anchoring strength. Shortly after desorption begins, the anionic form of *ortho*-methyl red experiences photoinduced adsorption back onto the surface, consistent with the results of other researchers. This is also confirmed by changes in the absorption spectra. Readsorbed anionic dye molecules are bound to the surface more strongly than before and our results show that they are not as easily desorbed when photoexcited. Anchoring strengths for the nematics doped with *ortho*-methyl red could not be determined, as a magnetic field not only applied a torque to the director, but also to the easy axis resulting in an elastic rotation of the easy axis.

These results lead us to propose the following mechanism for photoinduced reorientation of *azo* dye-doped nematics: Both neutral and anionic forms of the dye are initially adsorbed to the surface aligned with the easy axis as determined by the rubbing direction. The anionic form provides a negative surface charge responsible for a stable orientation of the nematic throughout the sample. When a pump beam is applied, dyes with transition dipoles more in alignment with the polarization of the light are preferentially photoexcited. Anionic forms of these dyes desorb, resulting in a depletion of anionic dye molecules aligned with the polarization of the pump beam and a nonsymmetric distribution of anionic dyes around the original easy axis. The result is a different easy axis rotated away from the polarization of the pump beam, but by no more than a few degrees. While this is the end of the story for *meta*- and *para*-methyl red, apparently *ortho*-methyl red in the bulk can ionize and adsorb back to the surface upon photoexcitation. These negatively charged dye molecules are adsorbed with an orientation more in line with the polarization of the pump beam. The result is rotation of the easy axis toward the polarization of the pump beam. This rotation can be quite large, as has been observed.

The elastic rotation of the easy axis observed when a magnetic field is applied only to *ortho*-methyl red, we believe, is the result of structural differences in the anionic form of the dyes. While the neutral forms of all three dyes are planar, the anionic forms only of *meta*- and *para*-methyl red are planar. The anionic form of *ortho*-methyl red has the carboxylated phenyl ring rotated out of the plane of the molecule by about 30°. We propose that this phenyl ring is rotated out of the polymer surface. The magnetic field applies a torque to this negatively charged phenyl ring, resulting in a rotation of the easy axis away from the magnetic field. When the magnetic field is removed, the phenyl ring returns to its original position, hence the elastic rotation of the easy axis. This does not occur with planar anionic *meta*- and *para*-methyl red dyes adsorbed to the surface. Within the bulk nematic, the torque applied by the magnetic field on the liquid crystal molecules rotates the director toward the magnetic field regardless of the *azo* dye.

ACKNOWLEDGMENTS

We gratefully acknowledge Dr. Mark Ams for his many helpful and stimulating discussions regarding azobenzene and stilbene. This material is based upon work supported by Allegheny College and by the National Science Foundation under Grant No. 0910758.

[1] I. Jánossy, Molecular interpretation of the absorption-induced optical reorientation of nematic liquid crystals, Phys. Rev. E **49**, 2957 (1994).

[2] L. Marrucci, D. Paparo, P. Maddalena, E. Massera, E. Prudnikova, and E. Santamato, Role of guest-host intermolecular forces in photoinduced reorientation of dyed liquid crystals, J. Chem. Phys. **107**, 9783 (1997).

[3] M. Kreuzer, E. Benkler, D. Paparo, G. Casillo, and L. Marrucci, Molecular reorientation by photoinduced modulation of rotational mobility, Phys. Rev. E **68**011701 (2003).

[4] M. Becchi, I. Jánossy, D. S. Shankar Rao, and D. Statman, Anomalous intensity dependence of optical reorientation in azo dye-doped nematic liquid crystals, Phys. Rev. E **69**, 051707 (2004).

[5] D. Statman, V. Basore, Y. Sulai, B. Dunlap, and I. Jánossy, Photoinduced gliding of the surface director in azo-dye doped nematic liquid crystals, Liquid Crytals **35**, 33 (2008).

[6] Yu. Kurioz, V. Reshetniak, and Yu. Reznikov, Orientation of a liquid crystal on a soft photoaligning surface, Mol. Cryst. Liq. Cryst. **375**, 535 (2002).

[7] O. Francescangeli, L. Lucchetti, F. Simoni, V. Stanic, and A. Mazzulla, Light-induced molecular adsorption and reorientation at polyvinylcinnamate-fluorinated/liquid-crystal interface, Phys. Rev. E **71**, 011702 (2005).

[8] D. Fedorenko, K. Slyusarenko, E. Ouskova, V. Reshetnyak, K. R. Ha, R. Karapinar, and Y. Reznikov, Light-induced gliding of the easy orientation axis of a dye-doped nematic liquid crystal, Phys. Rev. E **77**, 061705 (2008).

[9] D. Voloshchenko, A. Khyzhnyak, Y. Reznikov, and V. Reshetnyak, Control of an easy-axis on nematic-polymer interface by light action to nematic bulk, Jpn. J. Appl. Phys. **34**, 566 (1995).

[10] D. Fedorenko, E. Ouskova, V. Reshetnyak, and Y. Reznikov, Evolution of light-induced anchoring in dye-doped nematics: Experiment and model, Phys. Rev. E **73**, 031701 (2006).

[11] L. Lucchetti, L. Tifi, and F. Simoni, Director sliding induced by a circularly polarized light in dye-doped liquid crystals, Opt. Commun. **281**, 4363 (2008).
[12] D. Andrienko, V. Reshetnyak, Yu. Reznikov, and T. J. Sluckin, Nematic director slippage: role of angular momentum of light, Phys. Rev. E **63**, 011701 (2000).
[13] F. Simoni, L. Lucchetti, D. E. Lucchetta, and O. Francescangeli, On the origin of the huge nonlinear response of dye-doped liquid crystals, Opt. Express **9**, 85 (2001).
[14] E. Ouskova, Y. Reznikov, S. V. Shiyanovskii, L. Su, J. L.West, O. V. Kuksenok, O. Francescangeli, and F. Simoni, Photo-orientation of liquid crystals due to light-induced desorption and adsorption of dye molecules on an aligning surface, Phys. Rev. E **64**, 051709 (2001).
[15] A. V. Dubtsov, S. V. Pasechnik, A. D. Kiselev, D. V. Shmeliova, and V. G. Chigrinov, Electrically assisted light-induced azimuthal gliding of the nematic liquid-crystal easy axis on photoaligned substrates, Phys. Rev. E **82**, 011702 (2010).
[16] L. Lucchetti, M. Gentili, and F. Simoni, Colossal optical nonlinearity induced by a low frequency electric field in dye-doped liquid crystals, Opt. Express **14**, 2236 (2006).
[17] P. Pagliusi, B. Zappone, and G. Cipparrone, Molecular reorientation dynamics due to direct current voltage-induced redistribution in undoped nematic planar cell, J. Appl. Phys. **96**, 218 (2004).
[18] L. Lucchetti and F. Simoni, Role of space charges on light-induced effects in nematic liquid crystals doped by methyl red, Phys. Rev. E **89**, 032507 (2014).
[19] I. Jánossy, A. Vajda, and D. Statman, Influence of the molecular weight of a polymer on the gliding of nematic liquid crystals, Mol. Cryst. Liq. Cryst. **466**, 77 (2007).
[20] S. Faetti, M. Nobili, and I. Raggi, Surface reorientation dynamics of nematic liquid crystals, Eur. Phys. J. B **11**, 445 (1999).
[21] I. Jánossy and T. I. Kósa, Gliding of liquid crystals on soft polymer surfaces, Phys. Rev. E **70**, 052701 (2004).
[22] S. Joly, K. Antonova, Ph. Martinot-Lagarde, and I. Dozov, Zenithal gliding of the easy axis of a nematic liquid crystal, Phys. Rev. E **70**, 050701 (2004).
[23] A. Romanenko, V. Reshetnyak, I. Pinkevich, I. Dozov, and S. Faetti, Magnetic field induced director reorientation in the nematic cell with time-dependent anchoring due to adsorption/desorption of LC molecules, Mol. Cryst. Liq. Cryst. **439**, 1 (2005).
[24] S. V. Pasechnik, V. G. Chigrinov, D. V. Shmeliova, V. A. Tsvetkov, V. N. Kremenetsky, Liu Zhijian, and A. V. Dubtsov, Slow relaxation processes in nematic liquid crystals at weak surface anchoring, Liq. Cryst. **33**, 175 (2006).
[25] Y. Ouchi, M. B. Feller, T. Moses, and Y. R. Shen, Surface memory effect at the liquid-crystal-polymer interface, Phys. Rev. Lett. **68**, 3040 (1992).
[26] S.-K. Park, C. Lee, K.-C Min, and N.-S Lee, Structural and conformational studies of *ortho*, *meta*-, and *para*-methyl red upon proton gain and loss, Bull. Korean Chem. Soc. **26**, 1170 (2005).
[27] I. Jánossy, High-precision measurement of azimuthal rotational of liquid crystals on solid substrates, J. Appl. Phys. **98**, 043523 (2005).
[28] T.-C. Yu, Yu-L. Lo, and R.-R. Huang, Determination of azimuthal anchoring strength in twisted nematic liquid crystal cells using heterodyne polarimeter, Opt. Express **18**, 21169 (2010).
[29] J.-H. Zhang, Q. Liu, Y.-M. Chen, Z.-Q. Liu, and C.-W. Xu, Determination of acid dissociation constant of methyl red by multi-peaks Gaussian fitting method based on UV-visible absorption spectrum, Acta Phys. Chim. Sin. **28**, 1030 (2012).
[30] S. J. Khouri, I. A. Abdel-Rahim, E. M. Alshamaileh, and A. M. Altwaiq, Equilibrium and structural study of m-methyl red in aqueous solutions: distribution diagram construction, J. Solution Chem. **42**, 1844 (2013).